Achieving Epitaxy between Incommensurate Materials by Quasicrystalline Interlayers

K. J. Franke,[1] P. Gille,[2] K.-H. Rieder,[1] and W. Theis[1,*]

[1]*Institut für Experimentalphysik, Freie Universität Berlin, Arnimallee 14, 14195 Berlin, Germany*

[2]*Sektion Kristallographie, Ludwig-Maximilians-Universität München, Theresienstrasse 41, 80333 München, Germany*

(Received 4 December 2006; published 19 July 2007)

Epitaxial interfaces of commensurate periodic materials can be characterized by a *locking into registry* of their atomic structure. This characteristic is identified as a natural framework to capture the essence of epitaxy also for systems including quasicrystalline materials. The resulting general definition for epitaxy requires a matching of reciprocal lattice points. The consequences for the real space structure of an epitaxial interface between quasiperiodic and periodic materials are explored and an experimental realization of such an interface is presented. It is demonstrated that due to their higher number of reciprocal lattice basis vectors (exceeding three), quasicrystals can provide interlayers epitaxially linking incommensurate materials.

DOI: 10.1103/PhysRevLett.99.036103 PACS numbers: 68.35.Ct, 05.70.Np, 61.44.Br

Epitaxial interfaces are a fundamental building block in device technology. The epitaxial alignment yields interfaces with perfect long-range order. This homogeneity precludes intrinsic defects, which would degrade the devices by acting as charge carrier traps, scattering centers, or weak points in mechanical and chemical stability. However, if two half-crystals of periodic materials are incommensurate and thus cannot form a direct epitaxial interface, there is no possibility of connecting them in any type of epitaxial structure—even with interlayers—within the class of periodic materials. Here we show that quasiperiodic materials [1] can provide interlayers, which epitaxially mediate between incommensurate materials.

The general term epitaxy as first introduced by Royer in 1928 [2] describes macroscopic interfaces between single crystals exhibiting well-defined relative orientations. In thin film growth and device technology, epitaxial interfaces denote interfaces which are *locked into registry*. Within the class of periodic solids, these epitaxial interfaces can be characterized by the existence of a shared interface unit cell and are also referred to as commensurate. Since quasicrystals do not have a unit cell [1], we must choose a more fundamental starting point for the characterization of epitaxy including quasicrystals.

For this, we describe epitaxial interfaces based on the concept of *locking into registry* as follows: An infinitely extending interface between two half-crystals [3] is epitaxial if a suitable interface energy has a local minimum with regard to lateral shifts of one of the half-crystals with respect to the other [4]. For simplicity, initially we consider only a single plane of each of the two crystals, choose a general pairwise potential $V(\mathbf{r}_1 - \mathbf{r}_2)$ and a resulting interface energy of

$$E(\mathbf{r}_s) \propto \iint \rho_1(\mathbf{r}_1 - \mathbf{r}_S)\rho_2(\mathbf{r}_2)V(\mathbf{r}_1 - \mathbf{r}_2)d^2r_1 d^2r_2 \propto \int \hat{\rho}_1(-\mathbf{k})\hat{\rho}_2(\mathbf{k})\hat{V}(\mathbf{k})e^{-i\mathbf{k}\mathbf{r}_S}d^2k, \quad (1)$$

with $\rho_{1,2}(\mathbf{r})$ the atomic densities of the surfaces, $\mathbf{r}_S$ the lateral shift, and $\hat{\rho}_{1,2}(\mathbf{k})$ and $\hat{V}(\mathbf{k})$ the corresponding Fourier transforms. Crystals, including quasicrystals, have discrete diffraction patterns generated by a finite set of reciprocal lattice basis vectors. (If the number of basis vectors exceeds three, the crystal is quasicrystalline.) Since $\hat{\rho}_{1,2}(\mathbf{k})$ are only nonzero on the respective reciprocal lattices, the energy can be written as a sum over all reciprocal lattice vectors $\mathbf{G}$ common to both surfaces:

$$E(\mathbf{r}_s) \propto \sum_{\mathbf{G}} \hat{\rho}_1(-\mathbf{G})\hat{\rho}_2(\mathbf{G})\hat{V}(\mathbf{G})e^{-i\mathbf{G}\mathbf{r}_S}.$$

If there are no common lattice vectors aside from $\mathbf{G} = 0$, then the energy $E(\mathbf{r}_S)$ is constant, i.e., independent of the lateral shift of the two surfaces. Local minima in $E(\mathbf{r}_S)$, as required for epitaxy, are only possible if the common sublattice G includes at least two vectors $\mathbf{G}_{1,2} \neq 0$ which are not collinear. For bulk-truncated half-crystals, $\hat{\rho}(-\mathbf{k})$ can only be nonzero if $\mathbf{k}$ is the interface projection of a 3D reciprocal lattice vector. Thus, we arrive at the following result: An interface between two half-crystals is epitaxial if the projections of the crystals' reciprocal lattices onto the interface plane have at least two noncollinear vectors in common. Since we did not resort to periodicity in the derivation, this definition of epitaxy applies to all types of crystals, including quasicrystals.

For the special case of periodic crystals, this is a well-known alternative formulation equivalent to the established definition requiring the existence of a common real space interface unit cell [4]. This condition of a common interface unit cell for epitaxy of half-crystals of periodic materials separates these into distinct sets, such that any pair of half-crystals within a single set can form an epitaxial interface, while those from different sets cannot. Thus, within periodic materials, interlayers cannot overcome the boundaries between these sets.

Quasicrystals, however, transcend this separation into distinct sets and can thus mediate epitaxially between incommensurate half-crystals. Let us assume $\mathbf{G}^A_{1,2}$ and $\mathbf{G}^B_{1,2}$ are noncollinear pairs of surface projected reciprocal

lattice vectors of the two incommensurate half-crystals A and B, respectively. Adding another vector normal to the interface, we have a set of five vectors $\{\mathbf{G}_i\}$. A quasicrystal with reciprocal lattice basis $\{\mathbf{G}_i\}$ would clearly yield an interlayer with epitaxial interfaces to the two half-crystals A and B. Indeed, it is straightforward to construct a hypothetical quasicrystalline atomic structure for any arbitrary basis set $\{\mathbf{G}_i, i = 1, \ldots, N\}$ by a 3D cut through a periodic structure defined in N-dimensional space [1]. Thus, for any two arbitrary half-crystals a quasicrystalline structure can be constructed which would yield an epitaxial interlayer.

However, no epitaxial interface between periodic and quasiperiodic materials, as defined above, has been demonstrated experimentally up to now. While a number of studies have reported interfaces with a defined relative orientation [5–10], so far the favoring of selected orientations has always been due to either local matching of clusters, local symmetry at preferred nucleation sites, or long length-scale strain modulations localized at the interface (coincidence of reciprocal lattice *planes* [10]).

Here we show that AlAs islands grow epitaxially on decagonal $Al_{71.8}Ni_{14.8}Co_{13.4}$ quasicrystals (henceforth Al-Ni-Co). The atomic structure of Al-Ni-Co consists of quasicrystalline planes stacked periodically along the tenfold direction. The reciprocal lattice is generated by five basis vectors, the first four pointing to four corners of a regular pentagon ($|\mathbf{G}_{10000}| = \cdots = |\mathbf{G}_{00010}| = 1.024$ Å^{-1}) and a perpendicular fifth vector ($|\mathbf{G}_{00001}| = 1.540$ Å^{-1}) reflecting the periodic direction [11].

Al-Ni-Co was grown by the Czochralski method [12], and the tenfold Al-Ni-Co(00001) surface was prepared in ultrahigh vacuum by cycles of ion bombardment and annealing. Holding the Al-Ni-Co surface at 600–800 °C to ensure sufficient Al bulk diffusion, arsenic was evaporated from a Knudsen cell forming AlAs multilayer islands. These were characterized by high-resolution low energy electron diffraction (SPALEED) and He-atom diffraction (HAS). Details of the instrumentation are given in Ref. [13]. SPALEED [Figs. 1(b) and 1(c)] shows ten rotationally equivalent sets of intense spots uniformly shifting position in k space with electron energy in addition to very weak stationary spots originating from flat Al-Ni-Co(00001) clean surface areas [see Fig. 1(a)]. The gray scale diffraction intensity plot for the plane spanned by the Al-Ni-Co(00001) surface normal and the in-surface [10000] direction [Fig. 1(d)] reveals tilted diffraction rods as the origin for the shifting spots. These demonstrate the formation of facet planes inclined along the Al-Ni-Co[10000] equivalent directions. From this image a facet angle α of approximately 35° is apparent. By recording the specular (mirror) reflections in HAS from both the facets and the remaining flat surface areas in a common angular scan, the facet angle was determined with high precision, yielding $\alpha = (35.27 \pm 0.15)°$.

The reciprocal lattice of the facet's surface is that of a slightly distorted hexagonal AlAs(111) film [Fig. 1(f)].

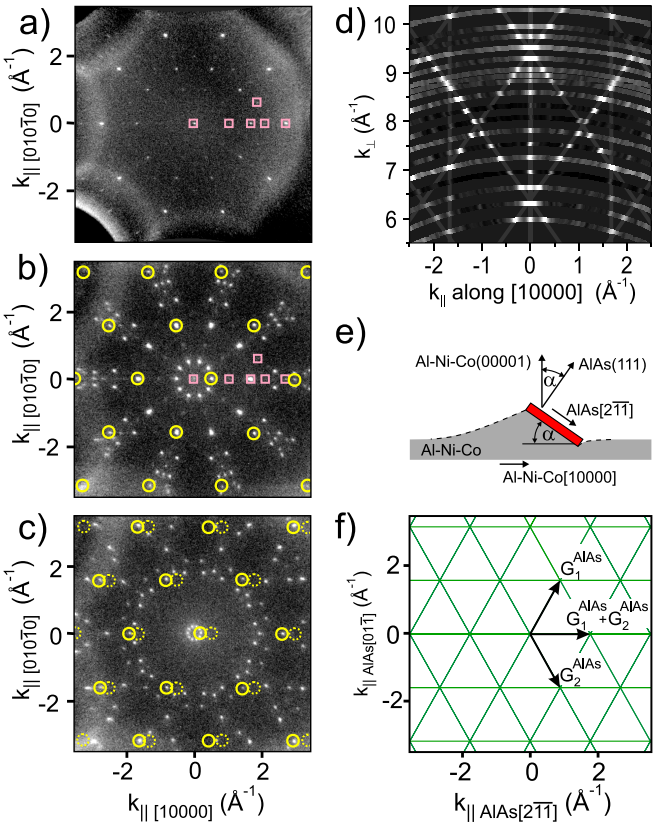

FIG. 1 (color online). (a) SPALEED pattern from Al-Ni-Co(00001) clean surface for electron energy $E_{kin} = 75$ eV, (b),(c) SPALEED pattern from epitaxial AlAs islands on Al-Ni-Co(00001) for $E_{kin} = 130$ and 140 eV, respectively. One of the ten symmetry related sets of facet spots is marked by circles, squares indicate clean surface peaks, dotted circles in (c) the locations of the corresponding facet spots in (b). (d) SPALEED intensity in the reciprocal space plane spanned by the in-surface [10000] direction and the surface normal; gray lines are guides to the eye. (e) Sketch of the derived geometry with faceted substrate [light gray, α is $(35.27 \pm 0.15)°$] and the in-plane orientation of the strained AlAs(111) film. (f) Surface reciprocal lattice of the strained AlAs(111) film (vertices of the grid: reciprocal lattice points).

The basis vectors $\mathbf{G}_{1,2}^{AlAs}$ are given by experimental values of $|\mathbf{G}_1^{AlAs} + \mathbf{G}_2^{AlAs}| = (1.774 \pm 0.010)$ Å^{-1} and $\mathbf{G}_{1,y}^{AlAs} := |\mathbf{G}_1^{AlAs} - \mathbf{G}_2^{AlAs}|/2 = (1.571 \pm 0.010)$ Å^{-1}. By comparing these to the corresponding AlAs bulk values of 1.812 and 1.569 Å^{-1}, respectively, we determine a unilateral strain of roughly 2% in the films. Based on this information, we can conclude that the Al-Ni-Co substrate has developed facets which are epitaxially overgrown by AlAs(111) films [14]. From the facet angle and facet directions we find that the facets are Al-Ni-Co(10$\bar{2}\bar{2}$4) and symmetry equivalent. [The angle between (10$\bar{2}\bar{2}$4) and (00001) is 35.15°.] The observed interface geometry is summarized in Fig. 1(e). The average facet size is at least 200 and 120 Å along and across the facet, respectively, as determined from the diffraction peak widths.

In order to demonstrate the epitaxial match at the interface, we compare the reciprocal lattice of the strained AlAs(111) film and the projection of the Al-Ni-Co reciprocal lattice onto the $(10\bar{2}\bar{2}4)$ plane in Fig. 2. One clearly observes a matching of the two reciprocal lattices. The common sublattice is identical to the reciprocal lattice of the AlAs(111) film. On the side of the quasicrystal it is generated by $\mathbf{G}_1 = P(\mathbf{G}_{110\bar{1}\bar{1}})$ and $\mathbf{G}_2 = P(\mathbf{G}_{0\bar{1}\bar{2}\bar{1}\bar{1}})$ where P denotes the projection of the Al-Ni-Co reciprocal lattice points onto the $(10\bar{2}\bar{2}4)$ interface plane. The values of $|\mathbf{G}_1 + \mathbf{G}_2| = 1.773$ Å^{-1} and $\mathbf{G}_{1,y} = |\mathbf{G}_1 - \mathbf{G}_2|/2 = 1.576$ Å^{-1} calculated using the Al-Ni-Co bulk lattice constants [15] are in perfect agreement with the experimentally determined reciprocal lattice vectors of the strained AlAs(111) film. This establishes that the AlAs(111)/Al-NiCo$(10\bar{2}\bar{2}4)$ interface is indeed epitaxial.

In order to gain an understanding of the atomic alignment at the epitaxial AlAs/Al-Ni-Co interface we will first consider a one-dimensional example matching a periodic with a quasiperiodic chain [Fig. 3(a)]. For the latter we choose a Fibonacci lattice [Fig. 3(a), small spheres). Its reciprocal lattice, shown in Fig. 3(b) by solid circles, is generated by two vectors G_{10} and $G_{01} = \tau G_{10}$ related by the golden mean $\tau = (1 + \sqrt{5})/2$. The diameters of the circles are proportional to the amplitudes of the Fourier component (structure factor) of the corresponding lattice vectors $G_{nm} = nG_{01} + mG_{10}$. The observed hierarchy in the structure factor amplitudes is a general feature in quasicrystals [1]. The periodic chain [Fig. 3(a), large spheres) was chosen to have its second order diffraction vector G_2 match $G_{11} = G_{10} + G_{01}$ of the Fibonacci chain. In Fig. 3(a), the lateral shift r_S between the chains was chosen such that all atoms keep a substantial lateral distance from the on-top sites. At different shifts the average lateral proximity of the atoms can be higher. [The highest proximity is attained by an additional shift of $\pm a/4$ in Fig. 3(a).] This variation of the atoms' lateral proximity yields a modulation of the interface energy $E(r_S)$, thus providing the locking into registry of the interface. While this variation in average proximity with r_S is apparent in the displayed section of the chains, we have to show that it is valid throughout the infinite chains. For this, we consider the average distribution $P(x)$ of the Fibonacci atoms within the unit cells of the periodic chain:

$$P(x) = \frac{1}{N}\sum_n \rho_{\mathrm{Fib}}(x - na) = \sum_m \hat{\rho}_{\mathrm{Fib}}(mG)e^{-imGx},$$

with $G = G_{11} = 2 \times 2\pi/a$ the basis vector of the common reciprocal sublattice [Fig. 3(c)] [16]. For a nonepitaxial interface only $G = 0$ would remain in the sum and thus $P(x)$ would be constant. For an epitaxial interface, $P(x)$ varies within the unit cell of the periodic chain, demonstrating the locking into registry of the infinite chains. As can be seen from the Fourier sum, the modulation of $P(x)$ is strong if the common sublattice includes quasicrystalline reciprocal lattice vectors with large structure factor $\hat{\rho}_{\mathrm{Fib}}(mG)$ (i.e., high diffraction intensity). Because, in the example, the common sublattice is generated by the second order of the periodic chain, two structurally and energetically equivalent interface alignments with a relative shift of $a/2$ exist. In film growth these would be observable as antiphase domains.

We will now apply the general understanding gained from the one-dimensional model to the AlAs films on Al-Ni-Co. The reciprocal lattice match depicted in Fig. 2 demonstrated that the common sublattice is identical to the AlAs(111) lattice, and one can further see that the rotational symmetry of the Al-Ni-Co$(10\bar{2}\bar{2}4)$ interface plane does not exceed that of AlAs(111). Thus, only a single domain with minimum energy is expected for an AlAs(111) film on a single Al-Ni-Co$(10\bar{2}\bar{2}4)$ terrace.

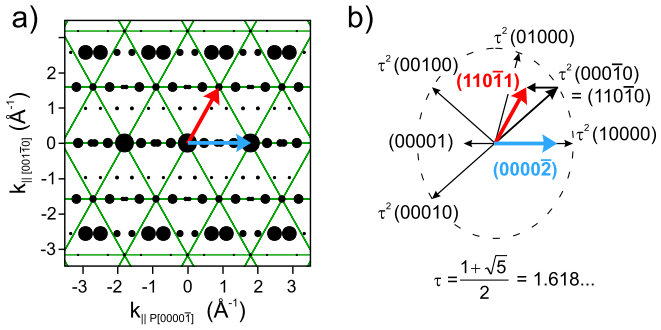

FIG. 2 (color online). (a) Reciprocal lattice match with circles depicting the reciprocal lattice of Al-Ni-Co projected onto the $(10\bar{2}\bar{2}4)$ interface plane and the vertices of the mesh of the AlAs(111) film. The radii of the circles are proportional to the Fourier amplitudes of the atomic density of Al-Ni-Co calculated from the structural model by Yamamoto and Weber [18]. (b) Projected Al-Ni-Co reciprocal lattice vectors.

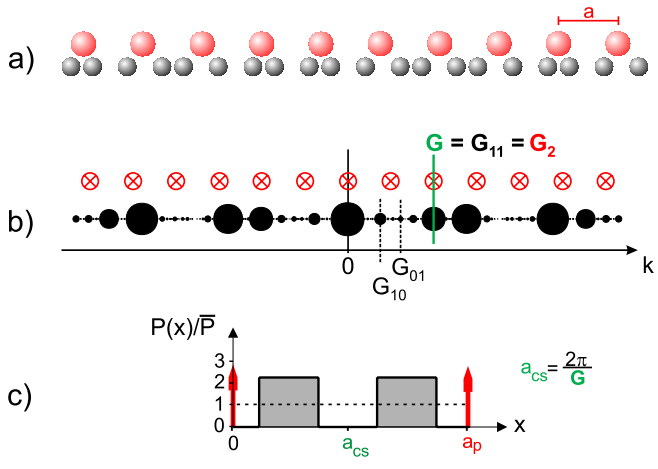

FIG. 3 (color online). Epitaxial interfaces between a periodic and a Fibonacci chain. (a) Real space structure for a repulsive interaction (disfavoring on-top sites). (b) Corresponding reciprocal lattice structure with the radii of the black circles proportional to the magnitude of the Fourier components. (c) Average distribution of the Fibonacci chain atoms within the unit cell of the periodic chain. The common reciprocal lattice vector is $G = G_{11}^{\mathrm{Fib}} = G_2 = 4\pi/a$.

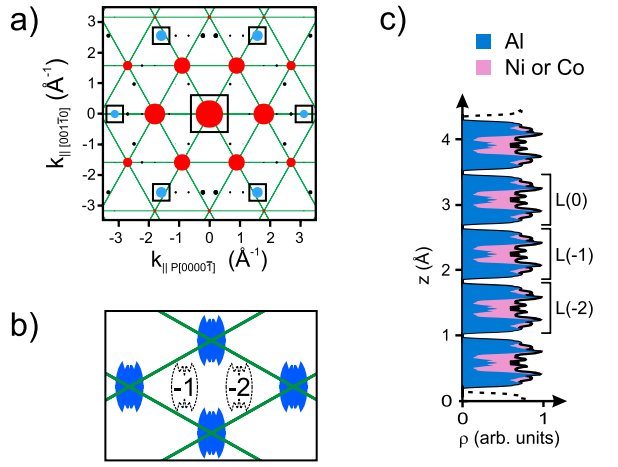

FIG. 4 (color online). Al-Ni-Co($10\bar{2}\bar{2}4$) surface layer atomic structure and structural match with AlAs(111). (a) Fourier transform of the top layer of bulk-truncated Al-Ni-Co($10\bar{2}\bar{2}4$), marked as L(0) in (c). The radii of the circles are proportional to the magnitude of the Fourier amplitudes. Circles at the vertices of the grid belong to the common sublattice. A strong set for potential alternate epitaxy is outlined by squares. (b) Average distribution of the atoms in the Al-Ni-Co interface layer L(0) in the real space interface unit cells of the AlAs(111) film. Those of the first and second Al-Ni-Co subsurface layers L(−1) and L(−2) are marked by dashed outlines. (c) Al-Ni-Co($10\bar{2}\bar{2}4$) areal atomic density $\rho(z)$ in the planes perpendicular to the [$10\bar{2}\bar{2}4$] direction. Calculations are based on the Al-Ni-Co structural model from Ref. [18].

The substantial strain necessary for the reciprocal lattice match can only be sustained by a strong chemical bonding at the interface. For this, a favorable alignment of the AlAs atoms with respect to the average Al-Ni-Co atomic distribution $P(\mathbf{r})$ within the unit cells of the AlAs film must be achieved. The distribution $P(\mathbf{r})$ is the extension of $P(x)$ to a two-dimensional interface, i.e., $P(\mathbf{r}) = 1/N\sum_{\mathbf{R}}\rho(\mathbf{r}-\mathbf{R})$, with the sum over all lattice vectors $\mathbf{R}$ of the periodic film and $\rho(\mathbf{r})$ the atomic density within the (suitably defined) top layer of the quasicrystalline surface. To define this top layer, we examine the areal atomic density $\rho_z(z)$ along the ($10\bar{2}\bar{2}4$) surface normal [Fig. 4(c)]. $\rho_z(z)$ is periodic due to the periodicity along the [00001] direction [17]. It exhibits segments of zero density every 0.83 Å [the periodicity of $\rho_z(z)$] and thus defines broadened atomic layers. The Fourier transform of an individual layer exhibits its strongest intensities on the common sublattice [Fig. 4(a)]. This is reflected in the strongly localized average atomic distribution $P(\mathbf{r})$ of the individual layers [Fig. 4(b)] and provides the basis for an excellent alignment and strong bonding between the atoms at the interface of AlAs(111) and Al-Ni-Co($10\bar{2}\bar{2}4$). The AlAs(111) surface top layer exhibits one atom per unit cell, corresponding to one atom per intersection of the green grid in Fig. 4(b). The Al-Ni-Co($10\bar{2}\bar{2}4$) layer, on the other hand, has its atoms strongly localized around a single site in the common unit cell, thus providing the potential for a strong modulation of the interface binding energy with respect to in-plane translation of the two sides of the interface against each other.

While for Al-Ni-Co($10\bar{2}\bar{2}4$) the lattice structure of AlAs(111) is clearly ideally suited for a strong epitaxial interface (see Fig. 4), other incommensurate strong sets of Fourier components also exist [e.g., marked spots in Fig. 4(a)]. These would allow an Al-Ni-Co($10\bar{2}\bar{2}4$) interlayer to mediate epitaxially between incommensurate materials.

In summary, we have derived a formulation for epitaxy extending the concept of commensurate interfaces to include quasiperiodic materials, illustrated its consequences for the real space structure at the interface, and presented an experimental realization of such an interface. The potential of quasicrystalline interlayers to epitaxially link incommensurate materials demonstrated in this Letter will allow the design of epitaxial structures incorporating functional units which up to now had been believed to be incompatible.

Support by the German Research Foundation under Grants No. Th732/2 and No. Gi211/3 is gratefully acknowledged.

*wolfgang.theis@physik.fu-berlin.de

[1] *Quasicrystals: An Introduction to Structure, Physical Properties, and Applications*, edited by J.-B. Suck, M. Schreiber, and Häussler (Springer, Berlin, 2002).
[2] L. Royer, Bull. Soc. Fr. Mineral. **51**, 7 (1928).
[3] Half-crystal: crystal cut parallel to a lattice plane.
[4] A. Zangwill, *Physics at Surfaces* (Cambridge University Press, Cambridge, England, 1990).
[5] Z. Shen *et al.*, Phys. Rev. B **58**, 9961 (1998).
[6] B. Bolliger *et al.*, Phys. Rev. Lett. **80**, 5369 (1998).
[7] M. Shimoda *et al.*, Phys. Rev. B **62**, 11 288 (2000).
[8] B. Bolliger *et al.*, Phys. Rev. B **63**, 052203 (2001).
[9] V. Fournée *et al.*, Phys. Rev. B **67**, 033406 (2003).
[10] E. J. Widjaja and L. D. Marks, Philos. Mag. Lett. **83**, 47 (2003); Phys. Rev. B **68**, 134211 (2003).
[11] W. Steurer *et al.*, Acta Crystallogr. Sect. B **49**, 661 (1993).
[12] B. Bauer *et al.*, Philos. Mag. **86**, 317 (2006).
[13] H. R. Sharma *et al.*, Phys. Rev. B **70**, 235409 (2004).
[14] Hut-shaped AlAs(110) on nonfaceted Al-Ni-Co(00001) can be ruled out, as this would yield a combination of AlAs-facet angle and facet strain which is inconsistent with the elastic response of the assumed AlAs island.
[15] $|\mathbf{G}_1 + \mathbf{G}_2| = |P(\mathbf{G}_{110\bar{1}\bar{1}} + \mathbf{G}_{0\bar{1}\bar{2}\bar{1}\bar{1}})| = |P(\mathbf{G}_{10222})| = |P(\mathbf{G}_{0000\bar{2}})| = 2|\mathbf{G}_{00001}|\sin(35.15°) = 1.773\ \text{Å}^{-1}$ and $\mathbf{G}_{1,y} = |\mathbf{G}_1 - \mathbf{G}_2|/2 = |P(\mathbf{G}_{110\bar{1}\bar{1}} - \mathbf{G}_{0\bar{1}\bar{2}\bar{1}\bar{1}})|/2 = |P(\mathbf{G}_{12200})|/2 = |\mathbf{G}_{12200}|/2 = |\mathbf{G}_{00100,y} + \mathbf{G}_{00100,y}| = [\sin(72°) + \sin(144°)] \times 1.024°\ \text{Å}^{-1} = 1.576°\ \text{Å}^{-1}$.
[16] $P(x)$ is closely related to the periodic average structure in W. Steurer and T. Haibach, Acta Crystallogr. Sect. A **55**, 48 (1999).
[17] W. Steurer and A. Cervellino, Acta Crystallogr. Sect. A **57**, 333 (2001).
[18] A. Yamamoto and S. Weber, Phys. Rev. Lett. **78**, 4430 (1997).